

Origins of Enantioselectivity during Allylic Substitution Reactions Catalyzed by Metallacyclic Iridium Complexes

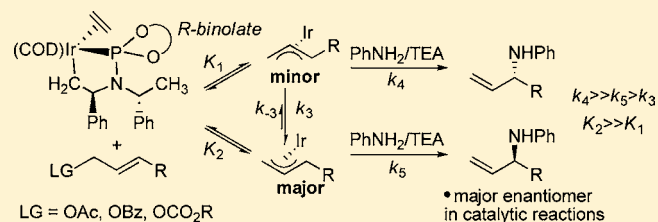
Sherzod T. Madrahimov[†] and John F. Hartwig^{*‡}

[†]Department of Chemistry, University of Illinois, 600 South Mathews Avenue, Urbana, Illinois 61801, United States

[‡]Department of Chemistry, University of California, Berkeley, Berkeley, California 94720-1460, United States

S Supporting Information

ABSTRACT: In depth mechanistic studies of iridium catalyzed regioselective and enantioselective allylic substitution reactions are presented. A series of cyclometalated allyliridium complexes that are kinetically and chemically competent to be intermediates in the allylic substitution reactions was prepared and characterized by 1D and 2D NMR spectroscopies and single-crystal X-ray diffraction. The rates of epimerization of the less thermodynamically stable diastereomeric allyliridium complexes to the thermodynamically more stable allyliridium stereoisomers were measured. The rates of nucleophilic attack by aniline and by *N*-methylaniline on the isolated allyliridium complexes were also measured. Attack on the thermodynamically less stable allyliridium complex was found to be orders of magnitude faster than attack on the thermodynamically more stable complex, yet the major enantiomer of the catalytic reaction is formed from the more stable diastereomer. Comparison of the rates of nucleophilic attack to the rates of epimerization of the diastereomeric allyliridium complexes containing a weakly coordinating counterion showed that nucleophilic attack on the less stable allyliridium species is much faster than conversion of the less stable isomer to the more stable isomer. These observations imply that Curtin–Hammett conditions are not met during iridium catalyzed allylic substitution reactions by $\eta^3\text{-}\eta^1\text{-}\eta^3$ interconversion. Rather, these data imply that when these conditions exist for this reaction, they are created by reversible oxidative addition, and the high selectivity of this oxidative addition step to form the more stable diastereomeric allyl complex leads to the high enantioselectivity. The stereochemical outcome of the individual steps of allylic substitution was assessed by reactions of deuterium-labeled substrates. The allylic substitution was shown to occur by oxidative addition with inversion of configuration, followed by an outer sphere nucleophilic attack that leads to a second inversion of configuration. This result contrasts the changes in configuration that occur during reactions of molybdenum complexes studied with these substrates previously. In short, these studies show that the factors that control the enantioselectivity of iridium-catalyzed allylic substitution are distinct from those that control enantioselectivity during allylic substitution catalyzed by palladium or molybdenum complexes and lead to the unique combination of high regioselectivity, enantioselectivity, and scope of reactive nucleophile.



I. INTRODUCTION

Iridium-catalyzed allylic substitution has become a powerful method for the enantioselective formation of both carbon–heteroatom^{1–8} and carbon–carbon^{9–15} bonds. The catalysts developed for this transformation (Figure 1) contain a diolefin ligand bound to a metallacyclic core that is formed by cyclometalation of an iridium–phosphoramidite complex in

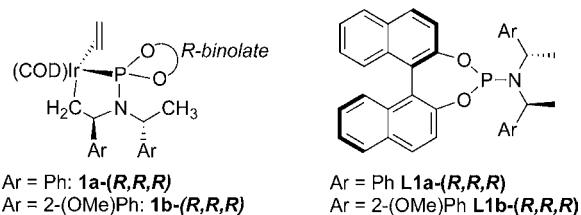


Figure 1. Catalysts and ligands commonly used for iridium catalyzed allylic substitution reactions.

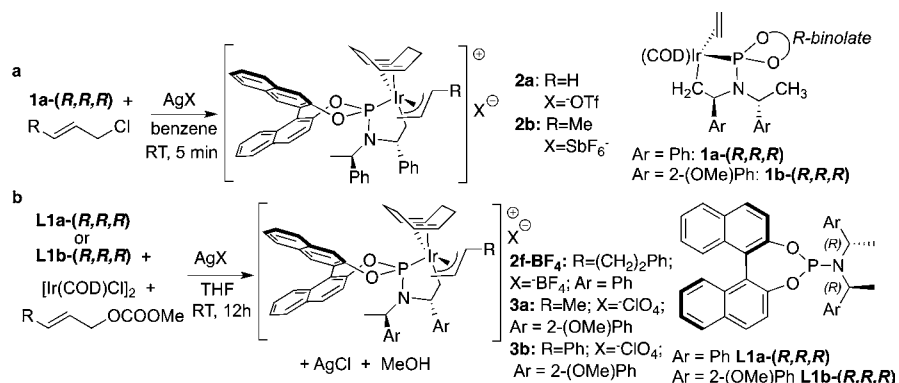
the presence of base.^{16,17} This class of catalyst converts linear allylic carbonates to substitution products with high regioselectivity for the branched isomers and with high enantiomeric excess. Recently, **1b** was also shown to be exquisitely selective for the conversion of one enantiomer of a racemic mixture of branched allylic benzoates to the allylic substitution products with overall retention of configuration. This reaction of racemic benzoates leads to high enantiomeric excess of both the substitution product and the unreacted ester.¹⁸

During the early mechanistic studies of iridium-catalyzed allylic substitution with catalysts derived from phosphoramidite ligands, the identity of the active species was revealed,¹⁹ and a catalytic cycle, along with information on relative rates and equilibria of the sequential steps, was deduced.²⁰ As part of these studies, a method for isolation and characterization of an allyliridium complex that is an intermediate in this reaction was

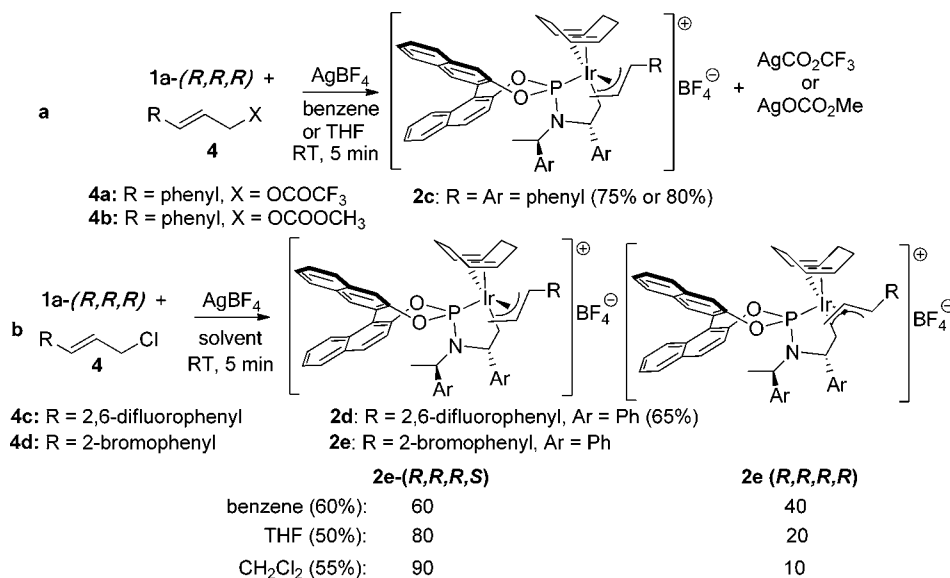
Received: December 31, 2011

Published: April 9, 2012

Scheme 1



Scheme 2



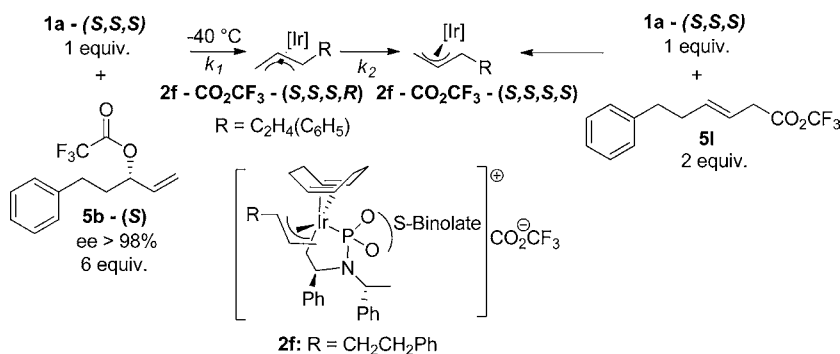
developed.¹⁶ Following this work, an alternative method for preparing analogous allyliridium complexes directly from $[Ir(COD)Cl]_2$ (COD = 1,5-cyclooctadiene) and the phosphoramidite ligand was published.²¹

Early studies on the stereochemical course of iridium-catalyzed allylic substitution showed that the overall reaction of 1-phenylallyl acetate or cyclic allylic carbonates occurs with predominant net retention of configuration when conducted with the combination of $[Ir(COD)Cl]_2$ and $P(O)Ph_3$ as catalyst precursors.^{9,22} This overall stereochemical outcome could result either from two steps occurring by inversion of configuration or from all steps occurring with retention of configuration. Reactions of substrates that discourage additions or eliminations with inversion of configuration with the catalyst derived from $[Ir(COD)Cl]_2$ and $P(O)Ph_3$ gave low yields of substitution product.²² However, these substrates are more sterically demanding than those commonly used in iridium-catalyzed allylic substitutions, and the catalyst contains a ligand that is much different from those now used most commonly for the iridium-catalyzed asymmetric allylic substitutions. Most important, little information on the origins of enantioselectivity has been gained during any of the prior studies. For example, the enantioselectivity-determining step of the catalytic cycle, the relative rates for epimerization of diastereomeric intermediates versus the reactions of the nucleophiles with

the allyl intermediates, the relative reactivity of the diastereomeric intermediates leading to different enantiomers of the substitution product, and the determination of the configurations of both intermediates and products that reveal the stereochemical outcome of individual steps of the catalytic cycle have not been determined.

We report the results of mechanistic studies conducted with catalysts containing cyclometalated phosphoramidite ligands that are the active form of the most commonly used iridium catalysts for allylic substitution. These studies provide information on (1) the stereochemistry of the individual oxidative addition and nucleophilic substitution steps; (2) isolation of the major allyliridium diastereomer in the catalytic cycle and direct observation of both major and minor diastereomers generated from alkyl- and aryl-substituted allylic electrophiles, and (3) the relative rates for epimerization of allyliridium complexes versus nucleophilic attack on the major and minor diastereomers. These studies provide deep-seated conclusions about the origins of the high stereoselectivity of iridium-catalyzed allylic substitution. Our data show that the factors controlling enantioselectivity in these iridium-catalyzed reactions are distinct from those controlling enantioselectivity in both palladium-catalyzed and molybdenum-catalyzed asymmetric allylic substitutions and that the relationships between diastereomeric intermediates and enantiomeric products are

Scheme 3



distinct from those of prior catalytic asymmetric systems studied mechanistically.

II. RESULTS AND DISCUSSION

1. Synthesis and Characterization of Allyliridium Complexes. Our previous studies showed that the stoichiometric reactions of allylic carbonates with the Ir(I) ethylene complex in Scheme 1 do not generate observable amounts of allyliridium complexes. Thus, we prepared allyliridium complex **2a** and crotyliridium complex **2b** previously by the route shown in part a of Scheme 1 involving the reaction of iridium–ethylene complex **1a**-(R,R,R), allyl or crotyl chloride, and silver salts containing non-coordinating anions.¹⁶ Subsequent work by Helmchen showed that crotyl complex **3a** and cinnamyliridium complex **3b** could be isolated from the route in part b of Scheme 1 starting from $[\text{Ir}(\text{COD})\text{Cl}]_2$, the phosphoramidite, allylic carbonates, and silver perchlorate.²¹ In addition, we prepared allyliridium complex **3b**, generated from ligand **L2**, by a procedure similar to that reported by Helmchen and co-workers.²¹ However, the mechanistic studies reported here required a route to allyliridium complexes that occurred under sufficiently mild conditions to observe directly both minor and major diastereomers containing the metal bound to the two different faces of the allyl unit.

After conducting further studies with allylic chlorides, we identified an alternative route to the allyl intermediates involving the reaction of iridium–ethylene complexes with allylic trifluoroacetates or with the combination of allylic carbonates and AgBF_4 (Scheme 2a). Both of these reactions allowed the isolation of pure allyliridium products in high yields and, in specific cases discussed later, as the mixtures of diastereomeric allyliridium complexes needed for the envisioned mechanistic studies. The reaction of ethylene complex **1a**-(R,R,R) with cinnamyl trifluoroacetate **4a** in THF, followed by the replacement of the trifluoroacetate anion by tetrafluoroborate anion, formed cinnamyliridium complex **2c** in 75% isolated yield. Similarly, reaction of the mixture of **1a**-(R,R,R) and methyl cinnamyl carbonate **4b** with AgBF_4 in THF led to the precipitation of silver methyl carbonate and formation of **2c** as the BF_4^- salt in 80% isolated yield. The substituted cinnamyliridium complex **2d** containing 2,6-difluoro substituents was prepared from the cinnamyl chloride (part b of Scheme 2).¹⁶ The reaction of **1a**-(R,R,R) with 2,6-difluorocinnamyl chloride **4c**, followed by exchange of the chloride anion by the tetrafluoroborate anion, gave allyliridium complex **2d** in 65% isolated yield.

As noted in the introduction to this section, the combination of ethylene complex **1a**-(R,R,R) and an excess amount of

methyl cinnamyl carbonate **4b** did not form the allyliridium complex in detectable quantities in the absence of AgBF_4 ;²⁰ **1a**-(R,R,R) remained unreacted. Thus, a small quantity of allyliridium complex formed in an unfavorable equilibrium appears to react irreversibly with AgBF_4 to form thermodynamically stable allyliridium complex with a non-nucleophilic counterion **2c**- BF_4^- , or the allylic carbonate is activated by association with the silver cation. The potential that the carbonate is activated by association with silver cation was tested by combining ethyl cinnamyl carbonate with AgBF_4 in $\text{THF-}d_8$ and comparing the ^1H NMR spectrum of the resulting solution with that of ethyl cinnamyl carbonate. No difference was observed between the two spectra, showing that little if any adduct is formed. A small amount of Lewis acid–base complex formed in an unfavorable equilibrium could be the species that reacts with the Ir(I) complex, but the absence of an observable adduct is at least consistent with reaction of the silver salt with a small amount of allyliridium carbonate complex.

Two synthetic routes provided access to samples of allyliridium complexes containing observable amounts of the less stable diastereomer. A mixture of diastereomers of cinnamyl complex **2e** was generated from reaction of 2-bromocinnamyl chloride, followed by addition of a silver salt containing a non-nucleophilic anion. Because ortho-substituted cinnamyl carbonates undergo iridium-catalyzed allylic substitution with lower enantiomeric excess than meta- or para-substituted cinnamyl carbonates (typically 70%–80% ee for 2-methoxy cinnamyl carbonates),^{1,8,15,23} we considered that the stoichiometric reaction of the Ir(I) species with an ortho-substituted allylic electrophile might generate a mixture of diastereomers. Indeed, reaction of the ethylene complex **1a**-(R,R,R) with 2-bromocinnamyl chloride, followed by addition of AgBF_4 , gave a mixture of diastereomers of **2e**. The ratios of diastereomers obtained from this process depended on solvent; preparation of **2e** in benzene gave a 60:40 ratio of diastereomers, preparation of **2e** in THF gave an 80:20 ratio of diastereomers, and preparation in CH_2Cl_2 gave a 90:10 ratio of diastereomers (part b of Scheme 2).

An alternative method to prepare a mixture of diastereomeric allyliridium complexes involves the reaction of one enantiomer of a branched allylic trifluoroacetate with the enantiomer of ethylene complex **1a** that generates the less stable diastereomeric allyl complex. As shown in Scheme 3, the reaction of the branched phenethyl-substituted allylic trifluoroacetic acid ester **5b**-(S)^{24,25} with ethylene-ligated iridium complex **1a**-(S,S,S) (Scheme 3) at -40 °C gave the less stable diastereomer **2f**-TFA-(S,S,S,R) of the corresponding allyliridium complex as the initial product of this oxidative addition. Over the course of

several hours at $-40\text{ }^{\circ}\text{C}$, **2f-TFA-(S,S,S,R)** converted to the more stable allyliridium diastereomer **2f-TFA-(S,S,S,S)**. When the same reaction between **5b-(S)** and **1a-(S,S,S)** was conducted at $25\text{ }^{\circ}\text{C}$, **2f-TFA-(S,S,S,R)** was not observed by NMR spectroscopy; the more stable allyliridium complex **2f-TFA-(S,S,S,S)** was formed quantitatively.

The new allyliridium complexes **2c**, **2d**, and **2e** prepared by the methods in Scheme 2, and the new complex **2f-BF₄** prepared as shown in Scheme 1, were characterized by multinuclear 1D and 2D NMR spectroscopy. Complexes **2c**, **2d**, and **2e** were also characterized by single-crystal X-ray diffraction analysis. The related complex **3b** was characterized by multinuclear 1D NMR spectroscopy. The ³¹P NMR spectrum of cinnamyliridium complex **2c** in THF-*d*₈ consisted of a single resonance at 118.5 ppm, consistent with the presence of a single observable diastereomer. Each of the ¹H NMR signals of the allylic protons of **2c** was well resolved. The chemical shifts of the allyl group are 5.61 ppm (substituted terminus), 4.85 ppm (proton on central allylic carbon), 2.83 ppm (*syn* proton on the terminal allylic carbon), and 2.05 ppm (*anti* proton on the terminal allylic carbon) in THF-*d*₈. Similarly, 2,6-difluorocinnamyliridium complex **2d** was characterized by ¹H NMR, ¹³C NMR, ³¹P NMR, and 2D gCOSY-NMR spectroscopy, as well as X-ray crystallography (*vide infra*). Again, a single ³¹P NMR resonance (115.6 ppm) was observed for samples in THF solvent. The ¹H NMR signals of the allylic protons for **2d** in THF-*d*₈ were also well-resolved and resonated at chemical shifts similar to those of the allyl group in **2c**. The solid-state structures of complexes **2c** and **2d** are shown in Figure 2. The ³¹P NMR spectrum of **2f-BF₄** consisted

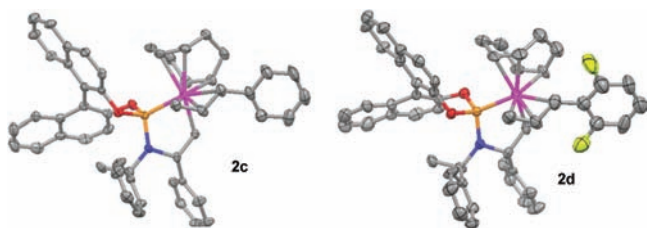


Figure 2. ORTEP diagrams of **2c** and **2d** (counterions and hydrogens are omitted for clarity; ellipsoids are drawn to 35% probability).

of a singlet at 120.6 ppm, and the ³¹P NMR spectrum of **3c** consisted of a singlet at 121.9 ppm which matches the value reported by Helmchen et al.²¹

The 2-bromocinnamyl complex **2e-BF₄** was characterized after synthesis in a solvent that favored one diastereomer, followed by recrystallization. Synthesis of 2-bromocinnamyl complex **2e-BF₄** in THF or CH₂Cl₂ from 2-bromocinnamyl chloride, ethylene complex **1a-(R,R,R)**, and AgBF₄, followed by recrystallization from benzene gave samples containing the two diastereomers with ratios as high as 95:5. The ³¹P NMR spectra of samples of **2e** consisted of two signals at 115.4 and 114.5 ppm for the major and minor diastereomers, respectively. The sample containing a 95:5 ratio of diastereomers was characterized by 1D ¹H NMR, 1D ¹³C NMR, and 2D gCOSY-NMR spectroscopy. The ratios of diastereomers of the 2-bromocinnamyl iridium complex **2e** generated in benzene, CH₂Cl₂, and THF were determined by ³¹P NMR spectroscopy. Preparation of **2e** in benzene and recrystallization from the same solution gave crystals containing an 80:20 ratio of diastereomers that were suitable for single-crystal X-ray diffraction (Figure 3). A ³¹P NMR spectrum of the individual

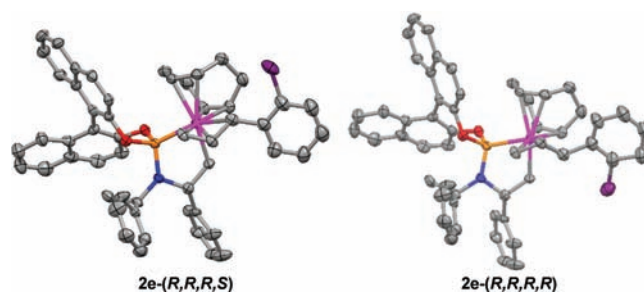


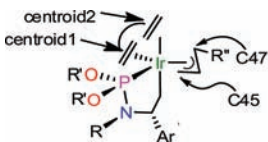
Figure 3. ORTEP diagrams of major and minor diastereomers of **2e** (counterions and hydrogens are omitted for clarity; ellipsoids are drawn to 35% probability) determined by X-ray diffraction of a crystal containing an 80:20 ratio of the major and minor diastereomers.

crystal was not obtained, but the same ratio of diastereomers was observed by ³¹P NMR spectroscopy of the bulk sample from which the crystal was selected for X-ray crystallography.

The identity of **2f-TFA-(S,S,S,R)** containing a phenethyl-substituted allyl group was deduced from several pieces of information. First, the ³¹P NMR spectra of the allyliridium complexes consist of singlets near 120–125 ppm, and a resonance assigned to **2f-TFA-(S,S,S,R)** was observed at 120.2 ppm. Second, the signal at 120.2 ppm decays as the intensity of the signal at 123.8 ppm increases. (The assignment of the ³¹P NMR resonance at 123.8 ppm to **2f-TFA-(S,S,S,S)** was corroborated by the reaction of **1a-(S,S,S)** with linear electrophile **5l** to form the same species, as shown in Scheme 3). Finally, studies described later in this paper show that oxidative addition of the allylic esters occurs with inversion of configuration, and the identity of **2f-TFA-(S,S,S,R)** as the kinetic product of oxidative addition is consistent with this inversion of configuration.

2. Structural Characterization of Cinnamyliridium **2c, 2,6-Difluorocinnamyliridium **2d**, and 2-Bromocinnamyliridium **2e**.** The solid-state structural data of the complexes **2c**, **2d** (Figure 2), and **2e-(R,R,R,S)** (Figure 3), as well as that of previously reported allyliridium complex **2a**, crotyliridium complex **2b**,¹⁶ and crotyliridium complex **3a** (which contains a phosphoramidite ligand with 2-methoxyphenyl groups **L1b**²¹) are listed in Table 1. An overlay of the structures of **2b** and **2c** is provided in Figure 4. The position of C47 (the carbon of the substituted allylic terminus) varies significantly among this series of compounds (Table 1 and Figure 4). The position of C45 (the carbon of the unsubstituted allylic terminus) varies to a lesser degree. More subtle differences are found in the bond angles, and these changes are analyzed in a footnote.²⁶ The Ir–C47 bond lengths increase with an increase in the size of the substituent on the allyl group, from 2.27 Å for parent allyliridium **2a** to 2.38 Å for crotyliridium **2b** and 2.32 Å for crotyliridium **3a** to 2.46 Å for cinnamyl, 2-bromocinnamyl, and 2,6-difluorocinnamyliridium complexes **2c–e**. Although large, this difference in metal–carbon bond lengths does not affect the other bond lengths around iridium; the other distances are within 0.05 Å of each other. Moreover, this difference in Ir–C47 distance does not lead to differences in the C–C bond lengths of the allyl unit that would reflect varying degrees of contribution of ene-yl resonance forms. As the difference between Ir–C47 and Ir–C45 bond lengths in the series of complexes increases from the small value of 0.07 Å for **2a** to the larger value of 0.14 Å for **2b** and 0.11 Å for **3a** and the largest value of 0.27 Å for **2c–e**, the C45–C46 bond lengths remain between 1.40 and 1.44 Å for all complexes, and the C46–C47

Table 1. Bond Distances and Angles around Ir for Allyliridium Complexes 2a–d,e-(R,R,R,S) and 3a



2a: Rⁿ = H, Ar = Ph
 2b: Rⁿ = Me, Ar = Ph
 2c: Rⁿ = Ph, Ar = Ph
 2d: Rⁿ = 2,6-difluorophenyl, Ar = Ph
 2e: Rⁿ = 2-bromophenyl, Ar = Ph
 3a: Rⁿ = Me, Ar = 2-(OMe)-C₆H₄

| | 2a | 2b | 2c | 2d | 2e-(R,R,R,S) | 3a |
|----------------|-----------|-----------|------------|------------|--------------|-----------|
| distances, Å | | | | | | |
| Ir–P | 2.2685(6) | 2.280(3) | 2.2582(14) | 2.2611(18) | 2.2633(14) | 2.248(4) |
| Ir–C45 | 2.204(3) | 2.240(10) | 2.190(5) | 2.191(6) | 2.209(6) | 2.21(2) |
| Ir–C47 | 2.274(3) | 2.377(11) | 2.461(5) | 2.460(7) | 2.445(6) | 2.319(17) |
| Ir–C21 | 2.125(3) | 2.114(15) | 2.120(5) | 2.111(6) | 2.120(5) | 2.124(12) |
| Ir–cent1 | 2.099 | 2.097 | 2.099 | 2.104 | 2.100 | 2.132 |
| Ir–cent2 | 2.244 | 2.215 | 2.263 | 2.258 | 2.264 | 2.211 |
| C45–C46 | 1.407(4) | 1.414(16) | 1.409(7) | 1.395(9) | 1.397(9) | 1.44(3) |
| C46–C47 | 1.405(4) | 1.39(2) | 1.387(7) | 1.368(9) | 1.396(8) | 1.40(2) |
| angles, deg | | | | | | |
| P–Ir–C45 | 86.96(8) | 85.9(3) | 85.28 | 85.2(2) | 85.83(17) | 90.2(6) |
| P–Ir–cent1 | 106.6 | 107.6 | 106.82 | 107.16 | 106.87 | 105.42 |
| cent1–Ir–C47 | 102.2 | 103 | 105.23 | 106.11 | 105.13 | 101.02 |
| C47–Ir–C45 | 66.4(1) | 66.0(5) | 63.2(3) | 62.3(3) | 62.8(2) | 66.3(8) |
| cent2–Ir–P | 103.8 | 104.6 | 103.22 | 103.82 | 102.92 | 104.65 |
| cent2–Ir–C45 | 90.0 | 90.9 | 94.26 | 92.65 | 94.34 | 88.74 |
| cent2–Ir–cent1 | 82.3 | 81.4 | 81.87 | 82.63 | 81.37 | 81.34 |
| cent2–Ir–C47 | 95.8 | 97.3 | 91.79 | 92.11 | 91.85 | 95.91 |
| C21–Ir–P | 75.73(8) | 75.0(4) | 76.39(14) | 75.94(18) | 76.59(15) | 73.7(4) |
| C21–Ir–C45 | 102.9(1) | 102.5(5) | 99.81 | 100.2(3) | 99.8(3) | 104.7(7) |
| C21–Ir–C47 | 90.9(1) | 89.9(5) | 96.09 | 95.2(3) | 96.1(2) | 91.6(6) |
| C21–Ir–cent1 | 85.6 | 86.4 | 84.7 | 85.06 | 85.20 | 86.03 |
| C45–C46–C47 | 121.3(3) | 127.5(3) | 122.1(2) | 121.2(2) | 122.1(4) | 121.8(17) |

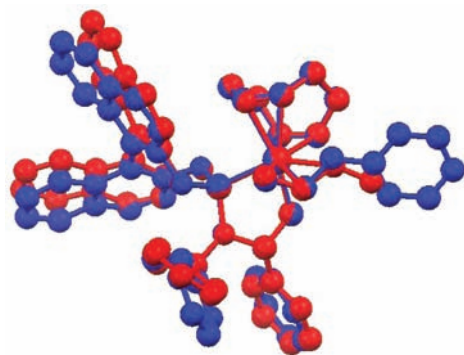


Figure 4. Overlay of solid state structures of 2b and 2c.

bond lengths remain between 1.39 and 1.41 Å, with one exception—the C46–C47 distance is only 1.368(9) Å for the 2,6-difluorocinnamyliridium complex 2d. This shorter C46–C47 bond length in 2e could be due to the presence of two strongly electron withdrawing units on the phenyl group, which would weaken the σ donation from the π system to the metal. Considering the proposed connection between the ene-yl form of an allyl unit and the regioselectivity for attack at the more substituted vs unsubstituted termini of an allyl group, the observation of high regioselectivity for formation of a branched isomer, despite the large changes in the difference between the two Ir–C bond lengths, is noteworthy. In addition, the structure of crotyliridium complex 3a is similar to that of crotyliridium complex 2b, which contains the phosphoramidite ligand L1a having plain phenyl groups, despite the often distinct reactivity and selectivity.

3. Kinetic Studies of the Reactions of the Allyliridium Complexes.

To elucidate the origin of enantioselectivity by the iridium catalyst in these substitution reactions, we measured the rate constants for epimerization of allyliridium complexes and the rate constants for nucleophilic attack on allyliridium complexes. Direct comparison of this set of rate constants would allow us to determine the enantioselectivity-determining step. Our synthetic route to a nonequilibrium ratio of diastereomeric allyl complexes allowed us to determine explicitly the values of these rate constants.

3a. Rates for Epimerization of Allyliridium Complexes. As described in section 1, the less thermodynamically stable allyliridium complex 2f-TFA-(S,S,S,R) was obtained by the oxidative addition of 5b-(S) (6 equiv) to 1a-(S,S,S) (Scheme 3). The conversion of 5b-(S) and 1a-(S,S,S) to the diastereomeric allyl complexes was monitored at –40 °C and at –30 °C. The initial >25:1 ratio of diastereomers of 2f favoring the less stable isomer 2f-TFA-(S,S,S,R) converts over the course of 5.5 h to a 5:3 ratio of diastereomers favoring the more stable isomer 2f-TFA-(S,S,S,S) and eventually leads to exclusive formation of thermodynamically favored 2f-TFA-(S,S,S,S). The rate constant for this isomerization process was assessed by monitoring the decay of the signal at 151.0 ppm in the ³¹P NMR spectrum of the initial reaction mixture, the changes in the intensity of the signal at 120.2 ppm for the less stable diastereomer, and the appearance of the signal at 123.8 ppm corresponding to the more stable diastereomer.

The plots showing the species present during the oxidative addition of 5b-(S) to 1a-(S,S,S) and during conversion of 2f-TFA-(S,S,S,R) to 2f-TFA-(S,S,S,S) at –40 °C are shown in Figure 5, and the plot corresponding to the same reaction

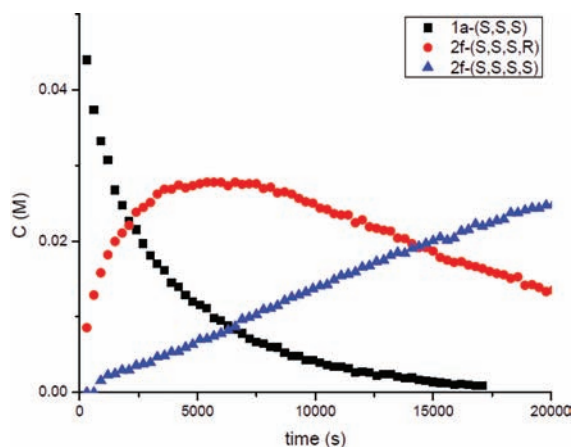


Figure 5. Plot of concentration vs time for the oxidative addition of **5b-(S)** to **1a-(S,S,S)** and isomerization of **2f-TFA-(S,S,S,R)** to **2f-TFA-(S,S,S,S)** at $-40\text{ }^{\circ}\text{C}$ in THF.

monitored at $-30\text{ }^{\circ}\text{C}$ is presented in the Supporting Information. This process follows a consecutive irreversible reaction sequence in which the two steps occur at similar rates.^{27,28} The decay of **1a-(S,S,S)** versus time corresponds to the oxidative addition of the branched allylic ester **5b-(S)** to **1a-(S,S,S)**. A large excess of allylic ester **5b-(S)** ensures that the oxidative addition occurs under pseudo-first-order conditions in **1a-(S,S,S)**. This process occurs with an exponential, first-order decay with a rate constant of $2.2 \times 10^{-4}\text{ s}^{-1}$ at $-40\text{ }^{\circ}\text{C}$ and with a rate constant of $5.8 \times 10^{-4}\text{ s}^{-1}$ at $-30\text{ }^{\circ}\text{C}$. These pseudo-first-order rate constants for oxidative addition (k_1) and the curve of **[2f-(S,S,S,R)]** versus time were used to determine the rate constant for isomerization of the allyliridium complex (k_2).

$$\frac{d[2f-(S, S, S, R)]}{dt} = k_1[1a-(S, S, S)] - k_2[2f-(S, S, S, R)] \quad (1)$$

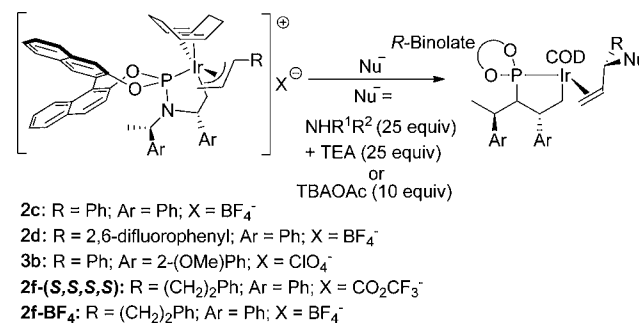
$$\frac{[2f-(S, S, S, R)]_{\max}}{[1a-(S, S, S)]_0} = \left(\frac{k_2}{k_1}\right)^{\frac{(k_2/k_1)}{1-(k_2/k_1)}} \quad (2)$$

The change in the concentration of **2f-TFA-(S,S,S,R)** over time is expressed in eq 1. Integration and approximation of eq 1, according to Swain's treatment,²⁷ gives eq 2. By iteratively fitting the experimental data to this equation, we determined that the rate constant for conversion of the minor to the major diastereomer is $5.4 \times 10^{-5}\text{ s}^{-1}$ at $-40\text{ }^{\circ}\text{C}$ and $3.4 \times 10^{-4}\text{ s}^{-1}$ at $-30\text{ }^{\circ}\text{C}$. Further details of this treatment of the data are provided in the Supporting Information.

3b. Rates of Nucleophilic Attack on the Allyliridium Complexes. The rate constants for nucleophilic attack on allyliridium complexes **2c**, **2d**, **2f-(S,S,S,S)**, and **3b** were determined by conducting reactions of the complexes with 25 equiv of a primary or a secondary amine nucleophile and 25 equiv of triethylamine as proton acceptor. The large excess of nucleophile creates pseudo-first-order conditions for the reaction of the nucleophile with the allyliridium complexes. Because the rate of these reactions surely depends on the concentration of nucleophile, it is important to consider the relative concentration of nucleophile in these stoichiometric reactions and a typical iridium-catalyzed allylic substitution reaction. The concentration of nucleophile in these stoichiometric reactions (0.75–1.15 M) is similar to that in the middle of a typical iridium-catalyzed allylic substitution (after one to

two half-lives).²⁹ Thus, the conclusions about the relative rates for nucleophilic attack on the allyl intermediate versus epimerization of the minor allyl diastereomer to the major diastereomer apply to the catalytic reactions. Moreover, data presented later in this paper imply that these relative rates are maintained throughout a catalytic reaction conducted under the standard conditions with a small excess of the nucleophile. The rate constants were determined by measuring the decay of the ³¹P NMR signal of the starting iridium complex. The reaction progress curves are provided in the Supporting Information, and the rate constants are provided in Table 2.

Table 2. Rate Constants of Nucleophilic Attack on Allyliridium Complexes 2c,d,f and 3b



| entry | complex ^a (M) | NHR ¹ R ² or TBAOAc | solvent | T, °C | k _{obs} s ⁻¹ |
|-------|----------------------------------|---|---------------------------------|-------|----------------------------------|
| 1 | 2c (0.030) | PhNH ₂ | CH ₂ Cl ₂ | -30 | 6.0 × 10 ⁻⁴ |
| 2 | 2c (0.043) | PhNH ₂ | THF | -40 | 3.4 × 10 ⁻³ |
| 3 | 2c (0.030) | PrNH ₂ | THF | -60 | too fast to measure |
| 4 | 2d (0.030) | PhNH ₂ | CH ₂ Cl ₂ | -30 | 2.8 × 10 ⁻⁴ |
| 5 | 2d (0.043) | PhNH(Me) | CH ₂ Cl ₂ | -30 | 2.0 × 10 ⁻⁴ |
| 6 | 3b (0.030) | PhNH ₂ | THF | -40 | 9.9 × 10 ⁻⁴ |
| 7 | 2c (0.030) | TBAOAc | THF | -60 | too fast to measure |
| 8 | 2f-TFA (0.046) | PhNH ₂ | THF | -40 | 2.5 × 10 ⁻³ |
| 9 | 2f-BF₄ (0.037) | PhNH ₂ | THF | -40 | 9.9 × 10 ⁻⁵ |

^aThe reactions of complexes **2c**, **2d**, **2f-BF₄**, and **3b** were conducted with the *R,R,R,R* diastereomers shown in the graphic. The reaction of **2f-TFA** was conducted with the *S,S,S,S* diastereomer.

The data in Table 2 reveal several trends: (1) The rate of nucleophilic attack is sensitive to the polarity of the solvent. A slight increase in the polarity of the solvent led to a large increase in the rate of nucleophilic attack (entry 1 vs entry 2). (2) Alkylamines react much faster than arylamines (entries 2 and 3). (3) *N*-Methylaniline and aniline react with nearly identical rate constants (entries 4 and 5). (4) Nucleophilic attack on cinnamyliidium complex **3b**, which bears the phosphoramidite ligand containing an anisyl group, is slower than nucleophilic attack on cinnamyliidium complex **2c** (entries 2 and 6), which bears the phosphoramidite ligand containing a phenyl group. This slower rate for attack on complex **3b** contrasts the often faster rate for catalytic allylic substitution with the anisyl-substituted system,^{8,30} suggesting that the origin of the difference in rate of the catalytic reactions as a function of the substituent on the phosphoramidite is more subtle than an effect on the rate of the turnover-limiting C–N bond-forming step within the catalytic cycle.

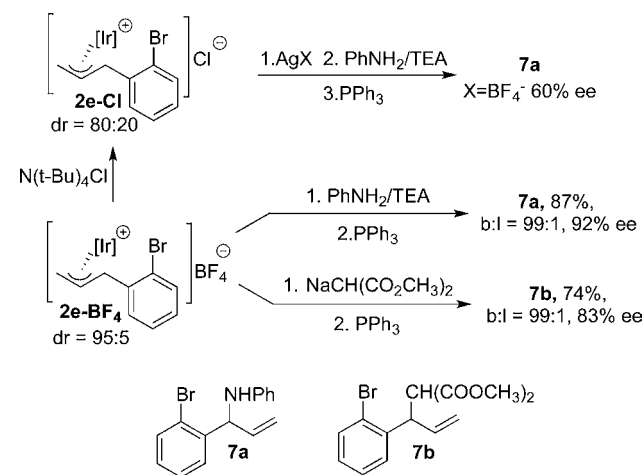
Most important for the current study is the conclusion one can draw by comparing the rate constants for interconversion of the diastereomeric allyliridium complexes with the rate constants for nucleophilic attack on allyliridium complexes. Nucleophilic attack of alkylamines on the allyliridium complexes was too fast to measure at $-60\text{ }^{\circ}\text{C}$ (Table 2: entry 3), whereas conversion of the minor to the major diastereomer of the allyliridium complexes required hours at $-40\text{ }^{\circ}\text{C}$. The rate constants for nucleophilic attack by arylamines in THF (Table 2, entries 2, 6, and 8) were found to be more than an order of magnitude larger than the rate constants for conversion of the minor to major diastereomers. For example, the rate constant for nucleophilic attack on the major diastereomer of **2f**-TFA-(*S,S,S,S*) was about fifty times faster than the $5.4 \times 10^{-5}\text{ s}^{-1}$ rate constant at $-40\text{ }^{\circ}\text{C}$ for epimerization of the minor diastereomer of **2f**-(*S,S,S,S*) deduced from the data in Figure 5. The rate constants for nucleophilic attack by arylamines on **2c** and **2d** in CH_2Cl_2 (Table 2, entries 1, 4, and 5) were found to be comparable to the rate constant for isomerization of the minor diastereomer of **2f** to the major diastereomer of **2f** at $-30\text{ }^{\circ}\text{C}$. The identity of the anion of the allyliridium complex had a strong influence on the rate of nucleophilic attack; more than an order of magnitude difference was observed between the rate constant for nucleophilic attack on **2f**-TFA and **2f**- BF_4 (Table 2, entries 8 and 9). Nucleophilic attack by acetate was too fast to measure at $-60\text{ }^{\circ}\text{C}$ (Table 2 entry 7). This final result agrees with our conclusion published previously in Communication form on the reactions of amines with allylic carbonates^{16,20} indicating that oxidative addition of allylic esters is reversible, as discussed further later in this Article.

These rate constants were measured at temperatures that were lower than those of the catalytic reactions conducted at room temperature. Thus, we determined the activation parameters for the nucleophilic attack of aniline on the major diastereomer of **2f**- BF_4 and extrapolated the rate constants to the $25\text{--}50\text{ }^{\circ}\text{C}$ temperatures of the catalytic reactions. Because data from the appearance and decay curves (Figure 5) would not give data sufficiently accurate for this analysis of the relative rates for epimerization and nucleophilic attack, we assessed the temperature dependence of this process by assuming that the entropy of activation for this intramolecular reaction was small. The details of the analysis can be found in the Supporting Information. This analysis shows that the rate for attack of aniline on the major diastereomer of the allyliridium complex **2f**-TFA is similar to the rate for epimerization of the minor diastereomer of **2f**-TFA to the corresponding major diastereomer.³¹ Because we showed that nucleophilic attack on the minor diastereomer is much faster than attack on the major diastereomer (*vide infra*), this analysis implies that nucleophilic attack on the minor diastereomer is faster than epimerization of the minor to major diastereomer. Moreover, we have shown that the major diastereomer is much more stable than the minor diastereomer, so the rate of conversion of the major diastereomer to the minor diastereomer is roughly 2 orders of magnitude or more slower than the rate of conversion of the minor diastereomer to the major diastereomer. Thus, attack of an arylamine on the major diastereomer should be faster than epimerization of this stereoisomer to the minor diastereomer under the catalytic conditions.

4. Reactions of Diastereomeric Allyliridium Complexes. *4a. Relationship between the Diastereomeric Excesses of the Allyliridium Complexes and the Enantiomeric*

Excesses of the Products of Nucleophilic Attack on the Allyliridium Complexes. The samples of 2-bromocinnamyliridium complex **2e** and phenethyl-substituted allyliridium complex **2f** containing mixtures of diastereomers allowed us to gain direct information on the relative rates for reaction of diastereomeric allyliridium complexes with an amine as nucleophile. The enantiomeric excesses from the reactions of mixtures of **2e**-(*R,R,R,S*) and **2e**-(*R,R,R,R*) with aniline and the sodium salt of dimethyl malonate are summarized in Scheme 4. The reaction of aniline with an 80:20 ratio of

Scheme 4. Stoichiometric Reactions of **2e**



diastereomers of **2e**- BF_4 generated by exchanging the chloride anion with a more weakly coordinating BF_4^- anion formed the *N*-phenyl allylic amine product in 60% ee. The enantioselectivity of this reaction corresponds precisely to the ratio of diastereomers. The reaction of aniline with a sample of complex **2e**- BF_4 consisting of a higher 95:5 ratio of diastereomers obtained after recrystallization from benzene formed the substitution product in a higher 92% ee. This enantioselectivity also corresponds well with the initial ratio of diastereomers in the sample of **2e**- BF_4 . When the same sample of **2e**- BF_4 consisting of a 95:5 ratio of diastereomers was allowed to react with sodium dimethylmalonate, the product of nucleophilic attack was formed in a slightly lower 83% ee, but this ratio of products (91.5:8.5 er) remains similar to the ratio of diastereomers. These results are consistent with the conclusion from kinetic measurements that the diastereomeric complexes **2e** containing noncoordinating anions react with the nucleophiles faster than they interconvert.

4b. Rate Constants for Reactions of Individual Diastereomeric Allyliridium Complexes with Amine Nucleophiles. The ability to generate mixtures of diastereomers that do not interconvert allowed us to measure directly the rate constants for reactions of the major and minor diastereomers of 2-bromocinnamyl complex **2e** with amine nucleophiles. The rates of these reactions were measured at $-60\text{ }^{\circ}\text{C}$ in CH_2Cl_2 . The data were collected with 10 equiv of PhNH_2 as nucleophile and triethylamine to quench the acid formed by the substitution process. We were unable to collect full reaction progress curves for nucleophilic attack on both diastereomers because the signal-to-noise ratio for the resonance of the minor isomer was low after the first half-life. However, we were able to gain information on the relative reactivity of the two diastereomers toward nucleophilic attack from the initial rates.

Plots showing the initial rates for reaction of the major and minor diastereomers are shown in Figure 6. The initial rate of

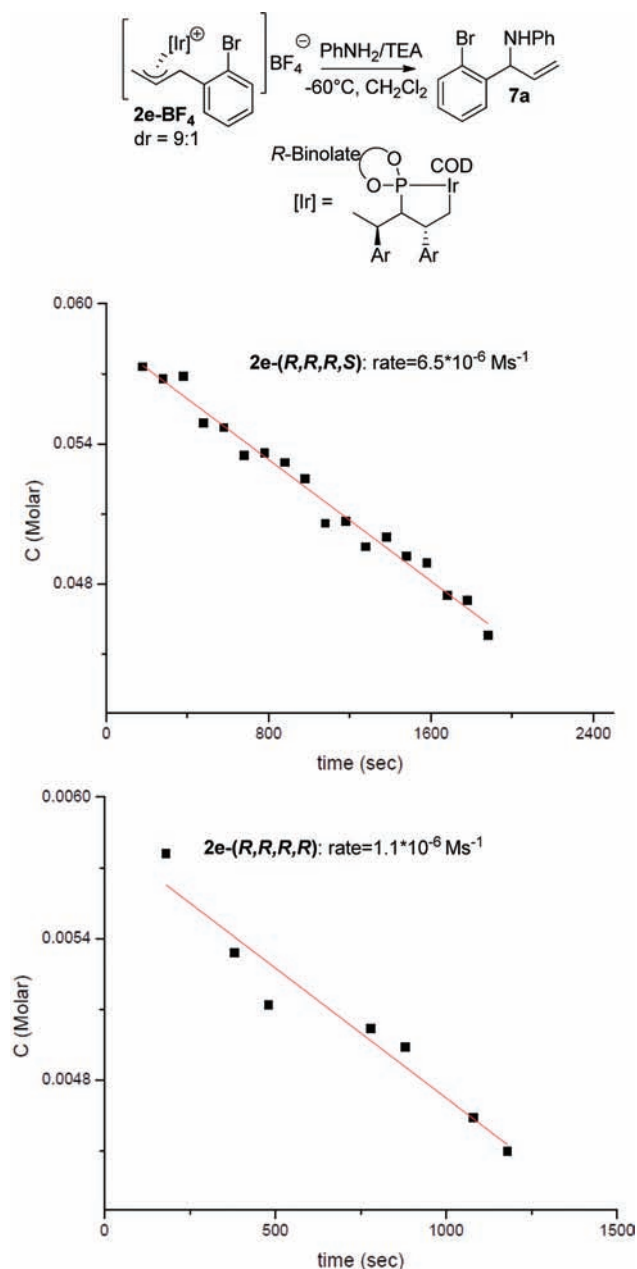


Figure 6. Initial rates of reaction of aniline with the major and minor diastereomers of **2e**-BF₄ at -60 °C.

reaction of the major diastereomer was $6.5 \times 10^{-6} \text{ M}\cdot\text{s}^{-1}$, and the initial rate of reaction of the minor diastereomer was $1.1 \times 10^{-6} \text{ M}\cdot\text{s}^{-1}$. The pseudo-first-order rate constants (k_{obs}) for the nucleophilic attack on each of the diastereomers can be calculated from these rates by dividing them by the initial concentrations of the two diastereomers. The two rate constants are $k_{\text{major}} = 1.2 \times 10^{-4} \text{ s}^{-1}$ and $k_{\text{minor}} = 2 \times 10^{-4} \text{ s}^{-1}$. These values calculated from initial rates show that the rate constant for reaction of the minor diastereomer is about two times larger than that for reaction of the major diastereomer when the reaction is conducted under the same conditions for both major and minor allyliridium complexes.

The similarity of these rate constants for nucleophilic attack on the two diastereomers (with reaction of the diastereomer that forms the minor enantiomer being slightly larger) suggests that the high enantioselectivity of the catalytic reaction must result from a highly selective oxidative addition of the allylic ester. This oxidative addition could be irreversible under the catalytic conditions, in which case the enantioselectivity would result from the kinetic ratio of diastereomers formed by this initial step, or it could be reversible under the catalytic conditions. In the latter case, Curtin–Hammett conditions would be established through reversible oxidative addition. We have shown that carboxylates react with the allyliridium intermediate to form free allylic esters,¹⁶ showing that the oxidative addition can be reversible (Table 2, entry 7). The reversibility of the oxidative addition step likely depends on the nucleophile. This step is clearly reversible for the reactions of amines, but it could be irreversible for reactions with anionic nucleophiles or reactions conducted with a precatalyst containing a weakly coordinating anion that would exchange with the carbonate anion.²¹ In either case, the enantioselectivity is based on a high stereoselectivity for oxidative addition, and this mode of enantioselection is different from that proposed to control enantioselectivity with palladium complexes that undergo facile η^3 - η^1 - η^3 interconversions.^{32,33}

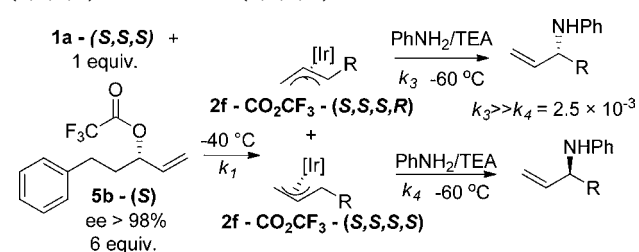
If the high enantioselectivity results from a high stereoselectivity for oxidative addition, then the catalytic reactions of 2-bromocinnamyl carbonates should occur with ee's that are modest (the stereoselectivity for oxidative addition is low, as described earlier in this paper). Consistent with this assertion, the reactions of 2-bromocinnamyl ethyl carbonate **6** with aniline, sodium dimethylmalonate, and lithium phenoxide catalyzed by **1a**-(*R,R,R*) form the substitution product with 25–29% ee (Table 3).³⁴

Table 3. Catalytic Reactions of 2-Bromocinnamyl Carbonate **6** with Aniline, Lithium Phenoxide, and Na-dimethylmalonate

| nucleophile (product) | yield, % | 7/8 | ee, % | T, °C | time, h |
|--|----------|------|-------|-------|---------|
| PhNH ₂ (7a) | 26 | 99:1 | 29 | 50 | 12 |
| (CH ₃ CO ₂) ₂ CHNa (7b) | 90 | 99:1 | 25 | RT | 12 |
| PhOLi (7c) | 53 | 99:1 | 26 | 50 | 0.5 |

We also sought to determine the relative rates for nucleophilic attack on the two diastereomeric allyl complexes in cases in which the enantioselectivity for the corresponding catalytic reaction was high. To do so, we measured the rates of nucleophilic attack on major and minor isomers of phenethylallyl complex **2f** (Scheme 5). A 1:1 ratio of **2f**-TFA-(*S,S,S,S*) and **2f**-TFA-(*S,S,S,R*) was generated by the reaction of Ir(I) ethylene complex **1a**-(*S,S,S*) and branched allylic trifluoroacetate **5b**-(*S*). Reactions of the two diastereomeric allyl complexes **2f** with aniline as nucleophile and triethylamine as proton acceptor revealed that the nucleophilic attack of aniline on **2f**-TFA-(*S,S,S,R*) is much faster than the

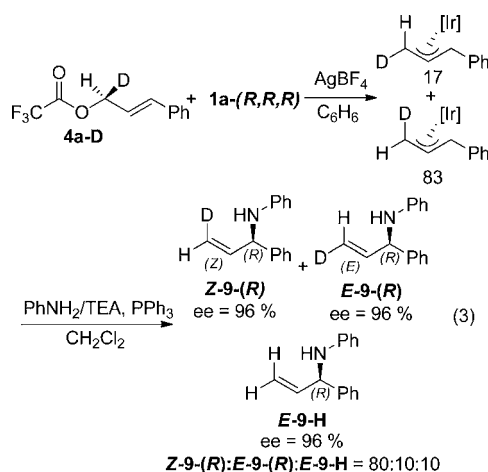
Scheme 5. Relative Rates of Nucleophilic Attack on 2f-TFA-(S,S,S,S) and 2f-TFA-(S,S,S,R)



nucleophilic attack on **2f**-TFA-(S,S,S,S) and that nucleophilic attack on both diastereomers is faster than interconversion of the two diastereomers containing the trifluoroacetate counterion (*vide supra*). The reaction of **2f**-TFA-(S,S,S,R) occurred to completion in less than 3 min at -60 °C, while the reaction of **2f**-(S,S,S,S) occurred to less than 5% conversion over the same time. The rate constant for nucleophilic attack by aniline on the more stable allyliridium diastereomer **2f**-(S,S,S,S) was determined quantitatively with the material prepared from the reaction of ethylene-ligated complex **1a**-(S,S,S) and linear allylic trifluoroacetate **5l** (Scheme 3). The rate constant at -40 °C in the presence of triethylamine as base was found to be $2.5 \times 10^{-3} \text{ s}^{-1}$ (Table 2, entry 8). The difference in rate constants for attack on these diastereomers is larger than that for attack on the 2-bromocinnamyl diastereomer and, again, favors formation of the minor enantiomer, but the stereoselectivity of the oxidative addition step is sufficiently high to cause the overall process to occur with high enantioselectivity.

5. Investigation of the Stereochemistry of the Individual Steps of the Catalytic Reaction. Prior studies of the stereochemistry of iridium-catalyzed allylic substitution reactions have shown that the reaction occurs with overall retention of configuration.^{9,22} To determine if this stereochemical outcome results from two steps of the catalytic cycle occurring by inversion of configuration or two steps occurring by retention of configuration, we determined the stereochemical changes that occur during the reaction of ethylene-ligated complex **1a**-(R,R,R) with an enantioenriched, deuterium-labeled linear allylic trifluoroacetate **4a-D**. In addition, we determined the stereochemical outcome of nucleophilic attack on the isolated allyliridium complexes that result from this oxidative addition. Finally, we conducted the reactions of enantioenriched, monodeuterated allylic carbonate **4b-D**²⁵ catalyzed by the two enantiomers of the cyclometalated iridium catalysts **1a** and **1b** to determine the relationship between the data gained on the stoichiometric reactions of the allylic trifluoroacetate and the data gained on the true catalytic system with allylic carbonates.

5a. Stoichiometric Reactions of the Ir(I) Ethylene Complex 1a-(R,R,R) with an Enantioenriched, Deuterium-Labeled Linear Allylic Trifluoroacetate and Reactions of the Addition Product with an Amine Nucleophile. The changes in configuration from the oxidative addition and reductive elimination steps were determined directly by conducting reactions of enantioenriched, monodeuterated, linear allylic trifluoroacetate **4a-D**-(S) (eq 3). The position of deuterium in the products of nucleophilic addition to these allyliridium complexes, coupled with the absolute configuration of the products, reveals the stereochemistry of the reaction of the allyl complex with nucleophiles. These studies are based on the system developed by Lloyd-Jones for determining the stereo-



chemistry of the individual steps of molybdenum-catalyzed allylic substitution reactions.^{25,35}

Reaction of the Ir(I) complex **1a**-(R,R,R) with the monodeuterated, enantioenriched cinnamyl trifluoroacetate **4a-D** (the enantiomeric ratio of the precursor alcohol was >95:5),^{24,35,36} followed by anion exchange with AgBF₄, formed an 83:17 ratio of allyliridium complexes containing the deuterium label *syn* and *anti* to the metal center, respectively (eq 3). The ratio of the complexes was determined by integration of the ¹H NMR signals corresponding to *syn* and *anti* protons at the terminal carbon of the allyl unit. This result is consistent with an oxidative addition process that occurs with inversion of configuration. The lack of exclusive formation of one stereoisomer is likely due to partial racemization of the substrate during esterification of the alcohol. We cannot determine the enantiomeric excess of the trifluoroacetate directly, but this result shows that the reaction occurs, at least predominantly, with inversion of configuration.

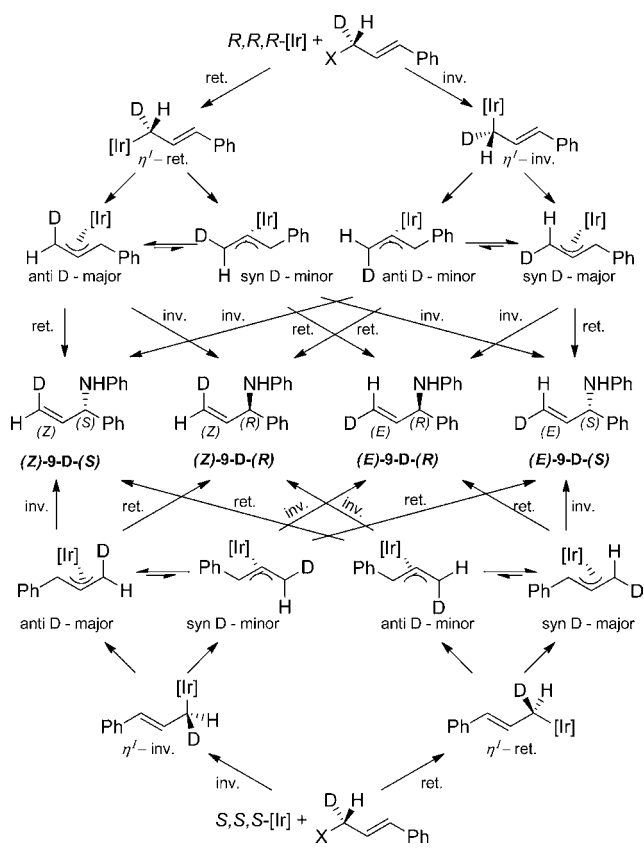
The stereochemistry of nucleophilic attack on the allyliridium intermediate was determined by reaction of aniline with the cinnamyliridium complex consisting of an 83:17 ratio of *syn* and *anti* isomers. This stoichiometric reaction gave the (R) enantiomer of the allylic substitution product **9** in 96% ee. The ratio of products **Z-9**-(R)/**E-9**-(R) was 8:1, with a small amount of product formed that lacked the deuterium label. This result is consistent with nucleophilic attack occurring with almost complete inversion of configuration. These two results show that the mechanism of iridium-catalyzed allylic substitution involves two inversions of configurations, one during oxidative addition of the allylic ester and one during reductive elimination that occurs by nucleophilic attack of the nucleophile on the allyl intermediate.

5b. Catalytic Reactions of Enantioenriched, Deuterium-Labeled Linear and Branched Allylic Electrophiles. Several differences between the stoichiometric reactions of section 5a and the catalytic system could compromise the conclusions drawn from the reactions of the trifluoroacetate. First, the stoichiometric reactions were conducted with the highly reactive cinnamyl trifluoroacetate **4a-D**, whereas catalytic reactions are typically conducted with the less reactive alkyl carbonates or acetates. Second, the stoichiometric reactions of the allylic electrophiles with amine and malonate nucleophiles were conducted with the cinnamyliridium complex containing a weakly coordinating BF₄⁻ counterion and with added amine as the proton acceptor, whereas the nucleophilic attack that takes place during the catalytic reactions occurs on an intermediate

containing either a carbonate, an acetate, or an alkoxide counterion without an external base.

Thus, we studied catalytic reactions of methyl cinnamyl carbonate **4b-D-(R)**, an enantioenriched, deuterium-labeled version of the allylic carbonate used in the catalytic process. This substrate was prepared from the enantioenriched, labeled allylic alcohol we had prepared for synthesis of the allylic trifluoroacetate. The potential products of the reactions of this labeled linear allylic carbonate are shown in Scheme 6.

Scheme 6



Oxidative addition with retention of configuration would generate the allyl intermediate with deuterium in the position *anti* to the central hydrogen of the allyl unit (labeled as *anti*-D-major), and oxidative addition with inversion of configuration would generate the allyl intermediate with deuterium in the position *syn* to the central hydrogen (labeled as *syn*-D-major). In addition, the minor allyliridium diastereomers similar to those of 2-bromocinnamyl and phenethyl-substituted allyl complexes **2e** and **2f**, respectively, can be formed (labeled as *anti*-D-minor and *syn*-D-minor) through η^3 - η^1 - η^3 interconversion. An interconversion from the η^3 form of *anti*-D-major to the η^1 isomer and back to the η^3 generates *syn*-D-minor, and an interconversion from the η^3 form of *syn*-D-major to the η^1 isomer and back to the η^3 form generates *anti*-D-minor. Nucleophilic attack with retention of configuration on the *anti*-D-major isomer shown would give (Z)-9-D-(S) as the organic product. Nucleophilic attack on *anti*-D-major with inversion of configuration would give (Z)-9-D-(R) as the major product.

The opposite outcome would be expected from nucleophilic attack on *anti*-D-minor. Nucleophilic attack on *anti*-D-minor with retention of configuration would give (Z)-9-D-(R), and nucleophilic attack on *anti*-D-minor with inversion of

configuration would give (Z)-9-D-(S). Similarly, two different products would form from nucleophilic attack on the *syn*-D-major and *syn*-D-minor allyliridium complexes. Nucleophilic attack on *syn*-D-major with retention of configuration would give (E)-9-D-(S) as the major product, and nucleophilic attack on *syn*-D-major with inversion would give (E)-9-D-(R) as the major product. Nucleophilic attack on *syn*-D-minor with retention would give (E)-9-D-(R) as the major product, and nucleophilic attack on *syn*-D-minor with inversion would give (E)-9-D-(S) as the major product.

Results from the catalytic allylic substitution of enantioenriched monodeuterated linear substrate **4b-D-(R)** are provided in Table 4. The reaction of **4b-D-(R)** with aniline catalyzed by

Table 4. Catalytic Reactions of Enantioenriched, Monodeuterated Allylic Carbonates with Aniline Catalyzed by Ethylene-Ligated Iridium Catalysts **1a and **1b****

| entry | catalyst | substrate | (Z)-9/(E)-9 | ee, % |
|-------|--------------------|-----------------|-------------|--------|
| 1 | 1a -(R,R,R) | 4b-D-(R) | 1:18 | 96 (R) |
| 2 | 1a -(S,S,S) | 4b-D-(R) | 18:1 | 96 (S) |
| 3 | 1b -(S,S,S) | 4b-D | 19:1 | 98 (S) |

1a-(R,R,R) gave (E)-9-D-(R) with 96% ee and a 18:1 ratio of *E*/*Z* isomers (Table 4: entry 1). The observed (R) and (E) configurations of the major product from the reaction catalyzed by the complex with (R,R,R) configurations is consistent with the sequence involving two inversions or two retentions (Scheme 6). The sequence involving two retentions can be ruled out, based on the outcome of the stoichiometric reactions (*vide supra*).

A similar stereochemical scenario can be proposed for the allylic substitution of the same monodeuterated, enantioenriched linear allylic electrophile **4b-D-(R)** with aniline catalyzed by the antipodal catalysts **1a** or **1b** possessing (S,S,S) absolute configuration. In this case, the opposite set of stereoisomers to those in Scheme 6 would be expected to form by each of the eight mechanisms. In that event, the reaction of **4b-D-(R)** with aniline catalyzed by **1a**-(S,S,S) gave the allylic substitution product (Z)-9-D-(S) with 96% ee and a 18:1 *Z*/*E* ratio (Table 4: entry 2), and the same reaction catalyzed by **1b**-(S,S,S) formed the substitution product (Z)-9-D-(S) with 98% ee and a 19:1 *Z*/*E* ratio (Table 4: entry 3). These results are also consistent with an iridium-catalyzed allylic substitution by the sequence involving two inversions. Thus, our data from the stoichiometric reaction and from the catalytic reaction are consistent with each other.

6. Comparison of the Origins of Enantioselectivity in Allylic Substitutions Catalyzed by Iridium, Palladium, and Molybdenum Complexes. The origins of enantioselectivity and the changes in configuration that occur during the iridium-catalyzed allylic substitution are distinct from those of catalysts based on complexes of the other metals most commonly used for allylic substitution. Most mechanistic studies have been conducted with palladium and molybdenum catalysts. The step that controls enantioselectivity is distinct from that of palladium systems, and the changes in configuration that occur during the molybdenum-catalyzed

reactions are different from those that occur during the iridium-catalyzed reactions.

Many versions of palladium-catalyzed asymmetric allylic substitution have been reported. In general, the configuration of the stereocenter formed at the allyl unit is controlled by the step involving nucleophilic attack on the coordinated ligand. Many palladium-catalyzed reactions involve intermediates containing symmetric allyl groups. In this case, the enantioselectivity is controlled by the relative rates for attack at one terminus of the allyl group over the other. In other cases, palladium-catalyzed reactions of linear or branched, mono-substituted allylic esters that form products from attack at the more substituted position of the allyl group occur with higher enantioselectivity when the rate of $\eta^3\text{-}\eta^1\text{-}\eta^3$ interconversions is faster than the rate of nucleophilic attack, presumably because the difference in rates of reactions of the diastereomeric allyl complexes is much larger than the equilibrium ratio of diastereomers.^{32,37,38} The rate of $\eta^3\text{-}\eta^1\text{-}\eta^3$ interconversions in palladium systems is typically faster than the rate of nucleophilic attack, most likely because the first step of this interconversion involves association of the counterion with the 16-electron metal center. In contrast to the mode of stereoselection proposed to apply to most palladium-catalyzed asymmetric allylic substitution reactions, the stereoselectivity of iridium-catalyzed allylic substitution originates from the oxidative addition step. The kinetic selectivity for formation of the more stable diastereomer and the relative ratios of the more stable diastereomer over the less stable diastereomer are both sufficiently high to compensate for the faster rate of attack of the nucleophile on the minor diastereomer. In these iridium-catalyzed allylic substitutions, nucleophilic attack on the minor diastereomeric allyl complex leads to the minor enantiomer of the organic product.

A series of asymmetric allylic substitutions also have been published with molybdenum catalysts,^{39–41} and many reactions with stabilized carbon nucleophiles occur with high enantioselectivity. Like the iridium-catalyzed allylic substitutions, the molybdenum-catalyzed reactions tend to form high ratios of branched to linear substitution products. Thus, one might expect that the origins of stereoselection by the two systems might be similar to each other. However, the studies we report on the changes in configuration during the iridium-catalyzed process show clearly that the iridium and molybdenum systems are distinct. The oxidative addition and reductive elimination steps of the molybdenum-catalyzed reaction occur with retention of configuration,²⁵ whereas these steps of the iridium-catalyzed process occur with inversion of configuration.

Finally, the relative rates for reactions of the diastereomeric intermediates in the iridium-catalyzed allylic substitutions are much different from those measured previously for asymmetric hydrogenation. The study by Halpern on the asymmetric hydrogenation of methyl acetamidocinnamate showed that the minor diastereomer formed the major enantiomer because the two diastereomers equilibrate and reaction of the minor diastereomer was several orders of magnitude faster than reaction of the major diastereomer.⁴² In contrast, Bergens has shown that the major diastereomer gives rise to the major enantiomer in ruthenium-catalyzed hydrogenations of ketones, and Curtin–Hammett conditions are not achieved because the formation of the hydrogenation product is faster than the interconversion of the diastereomeric intermediates.⁴³ For the iridium system that catalyzes allylic substitution analyzed in the current work, the minor diastereomer reacts faster than the

major diastereomer, but the major diastereomer forms the major enantiomer of the product. This scenario can occur in a system that leads to high enantioselectivity because the kinetic and thermodynamic selectivity for formation of the two diastereomers is even higher than the ratio of rate constants for reaction of the diastereomeric intermediates that favors formation of the minor enantiomer.

III. SUMMARY

Studies on the origins of stereoselectivity from iridium-catalyzed allylic substitution reactions showed that the factors controlling enantioselectivity are distinct from those of systems studied previously. These studies were enabled by the synthesis and characterization of a series of allyliridium complexes generated both as pure diastereomers and as mixtures of diastereomers. The following conclusions were drawn from our data.

- (1) The more stable diastereomer forms the major enantiomer of the organic product, but reaction of the more stable diastereomer is slower than reaction of the minor diastereomer. Thus, the oxidative addition of the allylic carbonate principally controls the enantioselectivity of the process.
- (2) Epimerization of the allyl intermediate containing a weakly coordinating anion occurs slowly, even at room temperature. This rate for epimerization is much slower than the rates for epimerization with palladium systems. This difference in rates of epimerization, most likely, results from a difference in coordination sphere. The iridium complex is a pseudo-octahedral, 18-electron d^6 system, a class of complex that typically undergoes ligand substitution by dissociative processes, while the palladium complexes are pseudo square-planar, 16-electron d^8 systems, which typically undergo ligand substitution by associative processes.
- (3) The rate for epimerization of individual diastereomeric allyliridium complexes containing weakly coordinating anions is slower than the rate for reaction of the respective diastereomers by attack of typical nucleophiles on the allyl group.
- (4) Equilibration of the diastereomeric allyliridium complexes likely occurs by reversible oxidative addition. Nucleophilic attack of carboxylate anions on the allyliridium intermediate is fast and thermodynamically downhill, making the oxidative addition process uphill and reversible.⁴²
- (5) The iridium-catalyzed allylic substitution occurs by an overall retention of configuration that results from two inversions. Oxidative addition of allylic esters occurs by inversion of configuration, and attack of the nucleophile on the allyl intermediate occurs by inversion of configuration. These changes in configuration during the reaction contrast those of the molybdenum system analyzed previously in a similar fashion.
- (6) The structures of the allyl intermediates containing different substituents on the allyl unit vary by the length of the metal–carbon bond to the substituted terminus, but this change in distance does not significantly affect the C–C bond distances, and the regioselectivity of the substitution process is high when the difference in M–C bond lengths is only 0.07 Å, as well as when this difference is over 0.27 Å.

Studies that further exploit these features of the catalytic system, studies that alter the relative rates by variations in the coordination sphere of the metal, and studies that reveal the factors that control the site-selectivity of these reactions are in progress.

■ ASSOCIATED CONTENT

■ Supporting Information

Experimental procedures for the synthesis of **2c**, **2d**, **2e**, and **2f**-**BF₄**, kinetic studies, and studies on the stereochemical outcome and catalytic reactions of 2-bromocinnamyl carbonate **5**; along with cif data. This material is available free of charge via the Internet at <http://pubs.acs.org>.

■ AUTHOR INFORMATION

Corresponding Author

jhartwig@berkeley.edu

Notes

The authors declare no competing financial interest.

■ ACKNOWLEDGMENTS

We thank the NIH (GM-55382) for support of this work and Johnson-Matthey for [Ir(COD)Cl]₂. We also thank Levi Stanley for helpful discussions.

■ REFERENCES

- (1) Ohmura, T.; Hartwig, J. F. *J. Am. Chem. Soc.* **2002**, *124*, 15164.
- (2) Shu, C.; Leitner, A.; Hartwig, J. F. *Angew. Chem., Int. Ed.* **2004**, *43*, 4797.
- (3) Pouy, M. J.; Leitner, A.; Weix, D. J.; Ueno, S.; Hartwig, J. F. *Org. Lett.* **2007**, *9*, 3949.
- (4) Yamashita, Y.; Gopalarathnam, A.; Hartwig, J. F. *J. Am. Chem. Soc.* **2007**, *129*, 7508.
- (5) Ueno, S.; Hartwig, J. F. *Angew. Chem., Int. Ed.* **2008**, *47*, 1928.
- (6) Pouy, M. J.; Stanley, L. M.; Hartwig, J. F. *J. Am. Chem. Soc.* **2009**, *131*, 11312.
- (7) Stanley, L. M.; Hartwig, J. F. *Angew. Chem.* **2009**, *121*, 7981.
- (8) Stanley, L. M.; Hartwig, J. F. *J. Am. Chem. Soc.* **2009**, *131*, 8971.
- (9) Takeuchi, R.; Kashio, M. *Angew. Chem., Int. Ed.* **1997**, *36*, 263.
- (10) Takeuchi, R.; Kashio, M. *J. Am. Chem. Soc.* **1998**, *120*, 8647.
- (11) Takeuchi, R. *Polyhedron* **2000**, *19*, 557.
- (12) Tissot-Croset, K.; Polet, D.; Alexakis, A. *Angew. Chem., Int. Ed.* **2004**, *43*, 2426.
- (13) Alexakis, A.; Polet, D. *Org. Lett.* **2004**, *6*, 3529.
- (14) Graening, T.; Hartwig, J. F. *J. Am. Chem. Soc.* **2005**, *127*, 17192.
- (15) Weix, D.; Hartwig, J. F. *J. Am. Chem. Soc.* **2007**, *129*, 7720.
- (16) Madrahimov, S. T.; Markovic, D.; Hartwig, J. F. *J. Am. Chem. Soc.* **2009**, *131*, 7228.
- (17) Kiener, C. A.; Shu, C.; Incarvito, C.; Hartwig, J. F. *J. Am. Chem. Soc.* **2003**, *125*, 14272.
- (18) Stanley, L. M.; Bai, C.; Ueda, M.; Hartwig, J. F. *J. Am. Chem. Soc.* **2010**, *132*, 8918.
- (19) Leitner, A.; Shekhar, S.; Pouy, M. J.; Hartwig, J. F. *J. Am. Chem. Soc.* **2005**, *127*, 15506.
- (20) Markovic, D.; Hartwig, J. F. *J. Am. Chem. Soc.* **2007**, *129*, 11680.
- (21) Spiess, S.; Raskatov, J.; Gnam, C.; Brödner, K.; Helmchen, G. *Chem.—Eur. J.* **2009**, *15*, 11087.
- (22) Bartels, B.; Garcia-Yebra, C.; Rominger, F.; Helmchen, G. *Eur. J. Inorg. Chem.* **2002**, *2002*, 2569.
- (23) Lopez, F.; Ohmura, T.; Hartwig, J. F. *J. Am. Chem. Soc.* **2003**, *125*, 3426.
- (24) Raminelli, C.; Comasseto, J. V.; Andrade, L. H.; Porto, A. L. M. *Tetrahedron: Asymmetry* **2004**, *15*, 3117.
- (25) Lloyd-Jones, G. C.; Krska, S. W.; Hughes, D. L.; Gouriou, L.; Bonnet, V. D.; Jack, K.; Sun, Y.; Reamer, R. A. *J. Am. Chem. Soc.* **2003**, *126*, 702.
- (26) The bond angles in the structures of allyliridium complexes **2a–e** involving C47 and C45 also change with substitution at the allyl terminus. The bond angle between cent1-Ir-C47 (centroid of the alkene unit cis to the allyl-Ir-branched allylic terminus) is 101–103 for **2a**, **2b**, and **3a** and 105–106 for **2c–e**. The C47-Ir-C45 angle which corresponds to the bite angle of the allyl unit is ~66 for **2a,b** and **3a** and 62–63 for **2c–e**. The angle between the Cent2 (centroid of the alkene unit in the axial position of the complex) and C45 (the unsubstituted terminus of the allyl unit) increases with increasing substitution on the allyl: the Cent2-Ir-C45 bond angle is 89–91 for **2a,b** and **3a** and 93–94 for **2c–e**. As a consequence, the angle between C21 (cyclometallated carbon) and C45 decreases in the series: C21–Ir–C45 bond angle is ~103 for **2a,b**, 105 for **3a**, and ~100 for **2c–e**. The opposite can be observed for the branched allylic terminus, where the bond angle between Cent2 (axial centroid) and C47 (branched allylic terminus) decreases with the size of substitution on the allyl: the Cent2–Ir–C47 bond angle is 96–97 for **2a,b**, **3a** and ~92 for **2c–e**. As a consequence, the angle between C21 (cyclometallated carbon) and C47 (branched terminus) increases in the series: the C21–Ir–C47 bond angle is 90–91 for **2a,b**, 92 for **3a**, and 95–96 for **2c–e**. These differences between the structures can also be seen in Figure 3. And finally, the angle between the allylic carbons C45–C46–C47 is 121–122 for **2a,c–e**, **3a** and 127.5(3) for **2b**.
- (27) Swain, C. G. *J. Am. Chem. Soc.* **1944**, *66*, 1696.
- (28) Neukom, J. D.; Perch, N. S.; Wolfe, J. P. *J. Am. Chem. Soc.* **2010**, *132*, 6276.
- (29) The initial concentration of amine in a typical iridium-catalyzed allylic substitution is 2–2.4 M.
- (30) Polet, D.; Alexakis, A. *Org. Lett.* **2005**, *7*, 1621.
- (31) See ref 29.
- (32) Mackenzie, P. B.; Whelan, J.; Bosnich, B. *J. Am. Chem. Soc.* **1985**, *107*, 2046.
- (33) Trost, B. M. *Chem. Pharm. Bull.* **2002**, *50*, 1.
- (34) As a side note, the yields of these reactions depended on the strength of the nucleophile. The reaction of aniline with **6** gave a 26% yield of product **7a**, whereas the reaction of lithium phenoxide gave the substitution product **7c** in 53% yield, and that of sodium dimethylmalonate gave the analogous product **7b** in 90% yield.
- (35) Malkov, A. V.; Gouriou, L.; Lloyd-Jones, G. C.; Stary, I.; Langer, V.; Spoor, P.; Vinader, V.; Kocovski, P. *Chem.—Eur. J.* **2006**, *12*, 6910.
- (36) This trifluoroacetate was prepared from the known labeled alcohol.
- (37) Hayashi, T.; Kawatsura, M.; Uozumi, Y. *Chem. Commun.* **1997**, 561.
- (38) Trost, B. M.; Toste, F. D. *J. Am. Chem. Soc.* **1999**, *121*, 3543.
- (39) Trost, B. M.; Miller, J. R.; Hoffman, C. M. *J. Am. Chem. Soc.* **2011**, *133*, 8165.
- (40) Belda, O.; Moberg, C. *Acc. Chem. Res.* **2004**, *37*, 159.
- (41) Trost, B. M.; Dogra, K.; Franzini, M. *J. Am. Chem. Soc.* **2004**, *126*, 1944.
- (42) Halpern, J. *Science* **1982**, *217*, 401.
- (43) Daley, C. J. A.; Bergens, S. H. *J. Am. Chem. Soc.* **2002**, *124*, 3680.